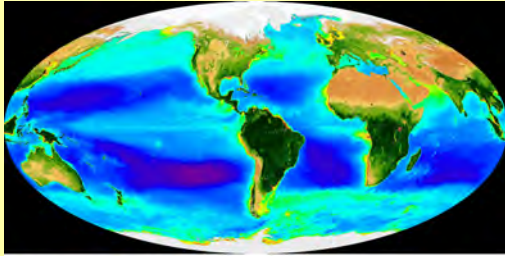


<div data-bbox="280 273 735 319" data-label="Section-Header"> <h2>Satellite Remote Sensing</h2> </div> <div data-bbox="337 323 672 354" data-label="Text"> <p>Class 28, Th 11 December 2008</p> </div> <div data-bbox="531 497 789 543" data-label="Image"> </div>	<div data-bbox="815 132 1273 174" data-label="Section-Header"> <h3>Slide 1 Satellite Remote Sensing</h3> </div> <div data-bbox="815 256 941 294" data-label="Text"> <p>NOTES:</p> </div>
<div data-bbox="284 653 742 701" data-label="Section-Header"> <h2>California Current System</h2> </div> <div data-bbox="311 707 709 741" data-label="Text"> <p>CZCS Image: Red Indicates high Chl <i>a</i></p> </div> <div data-bbox="269 743 542 1020" data-label="Figure"> </div> <div data-bbox="544 753 693 783" data-label="Caption"> <p>1981 CZCS Chl <i>a</i></p> </div> <div data-bbox="584 802 724 972" data-label="Figure"> </div> <div data-bbox="581 978 716 1024" data-label="Caption"> <p>Baja: SeaWiFS Chl <i>a</i></p> </div>	<div data-bbox="815 621 1304 663" data-label="Section-Header"> <h3>Slide 2 California Current System</h3> </div> <div data-bbox="815 743 941 781" data-label="Text"> <p>NOTES:</p> </div>
<div data-bbox="292 1142 734 1190" data-label="Section-Header"> <h2>Baja California upwelling</h2> </div> <div data-bbox="407 1190 596 1220" data-label="Text"> <p>Sea-surface Chl <i>a</i></p> </div> <div data-bbox="243 1213 600 1505" data-label="Figure"> </div>	<div data-bbox="815 1108 1294 1150" data-label="Section-Header"> <h3>Slide 3 Baja California upwelling</h3> </div> <div data-bbox="815 1230 941 1268" data-label="Text"> <p>NOTES:</p> </div>

SeaWiFS remote sensing of Chl a

<http://oceancolor.gsfc.nasa.gov/SeaWiFS/>



Northern Hemisphere, Fall & Winter

Slide 4 SeaWiFS remote sensing of Chl a

NOTES:

Remote sensing concepts

Satellite remote sensing of Chl a and production

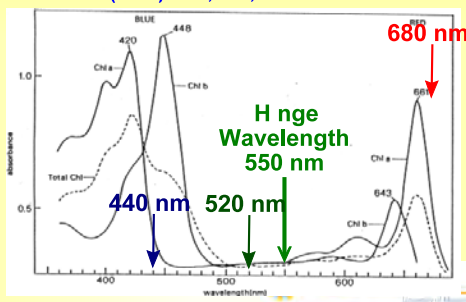
- How to estimate Chl a from space
 - CZCS, SeaWiFS & MODIS scanners
 - Type I (low Chl a) and Type II (high Chl a) algorithms
- Problems in estimating Chl a from space
- How to estimate production from space
 - Changes in Chl a within a water mass
 - Eppley *et al.* (1985) regression approach
 - Platt (1986) [Cole-Cloern] Ψ approach
 - Platt & Sathyendranath P vs. I approach
 - Behrenfeld & Falkowski VGPM estimates of production
 - Implemented by Oregon State
 - <http://web.science.oregonstate.edu/ocean.productivity/>

Slide 5 Remote sensing concepts

NOTES:

The CZCS Chl a algorithm

Brown *et al.* (1985): 440, 520, 550 and 680 nm sensors



Slide 6 The CZCS Chl a algorithm

NOTES:

SeaWiFS sensors

Joint & Groom (2000, JEMBE)

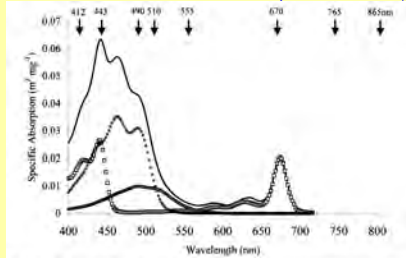


Fig. 1. Specific absorption due to all pigments (—), chlorophyll *a* (---), chlorophyll *b* (···) and phaeophytin (— · —) data published from Adams et al. (1993). The wavelengths of the SeaWiFS channels are indicated.

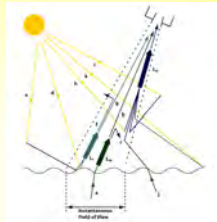
Slide 7 SeaWiFS sensors

NOTES:

Problems for Remote Sensing

Sensors detect to ≈ 1 optical depth

- Sensors detect only to 1 optical depth
 - Subsurface chlorophyll maxima never detected
- Cyanobacterial accessory pigments absorb at 550 nm
- Coccolithophorid blooms

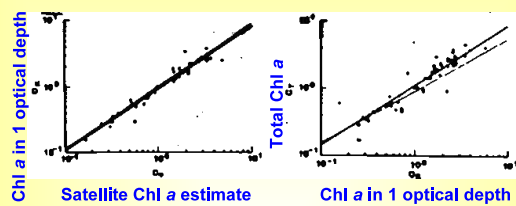


Slide 8 Problems for Remote Sensing

NOTES:

Estimating water-column Chl *a*

Eppley et al. (1985): note log-log scale



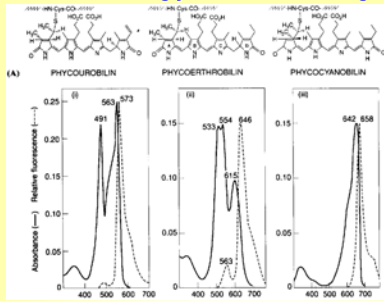
Optical depth = $1/k$, with k for PAR

Slide 9 Estimating water-column Chl *a*

NOTES:

Cyanobacterial phycobiliproteins

Absorb strongly at 550 nm, the 'hinge' wavelength



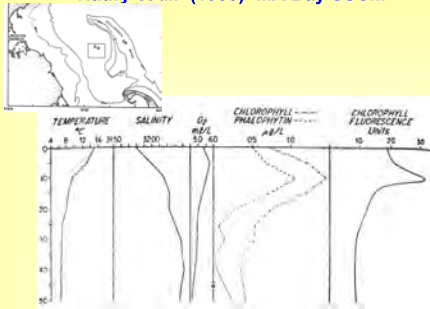
Cyanobacterial blooms could have been missed by the older CZCS algorithm

Slide 10 Cyanobacterial phycobiliproteins

NOTES:

SSCM usually at 4-5 optical depths

Haury *et al.* (1983): MA Bay SSCM



Slide 11 SSCM usually at 4-5 optical depths

NOTES:

Coccoliths reflect 550 nm light

From Newell & Newell (1973) & Valiella (1984, p. 1,4)

25 μm, A. coccolith

Slide 12 Coccoliths reflect 550 nm light

NOTES:

Eugene Gallagher © 2010

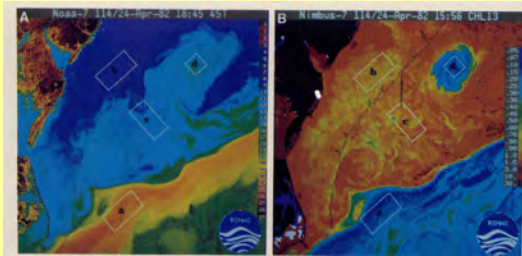
Page 4 of 14

ocw.umb.edu

<div data-bbox="326 168 699 205" data-label="Section-Header"> <h3>Coccolithophorid blooms</h3> </div> <div data-bbox="289 216 725 243" data-label="Section-Header"> <h4>Bering & Celtic Sea SeaWiFS True color images</h4> </div> <div data-bbox="274 241 466 480" data-label="Image"> </div> <div data-bbox="240 474 477 567" data-label="Text"> <p>http://oceancolor.gsfc.nasa.gov/SeaWiFS/BACKGROUND/Gallery/beringsea.jpg</p> </div> <div data-bbox="506 241 750 459" data-label="Image"> </div> <div data-bbox="503 459 782 516" data-label="Text"> <p>http://oceancolor.gsfc.nasa.gov/SeaWiFS/BACKGROUND/Gallery/celticsea.jpg</p> </div>	<div data-bbox="816 134 1297 172" data-label="Section-Header"> <h3>Slide 13 Coccolithophorid blooms</h3> </div> <div data-bbox="816 258 940 291" data-label="Text"> <p>NOTES:</p> </div>
<div data-bbox="263 655 779 695" data-label="Section-Header"> <h3>Estimating production from space</h3> </div> <div data-bbox="404 701 609 728" data-label="Section-Header"> <h4>Different approaches</h4> </div> <div data-bbox="235 728 751 980" data-label="List-Group"> <ul style="list-style-type: none"> • Directly estimate changes in Chl <i>a</i> concentration from different images • Regress primary production vs. Chl <i>a</i> (Smith <i>et al.</i> 1982, Eppley <i>et al.</i> 1985, Perry 1986) • Biooptical models: <ul style="list-style-type: none"> ▶ Include I_p and an estimate of water-column average quantum yield ψ 'psi' (Eppley <i>et al.</i> 1985, Platt 1986) ▶ Platt & Sathyendrenath (1988): include SSCM ▶ Behrenfeld & Falkowski VGPM model & Howard-Yoder models (differ in estimating mixed-layer depth) ▶ Behrenfeld <i>et al.</i> (2005): Carbon-based models & phytoplankton physiology from space (Global Biogeochemical Cycles 19: 1006) </div> <div data-bbox="529 987 786 1029" data-label="Image"> </div>	<div data-bbox="816 623 1424 661" data-label="Section-Header"> <h3>Slide 14 Estimating production from space</h3> </div> <div data-bbox="816 745 940 779" data-label="Text"> <p>NOTES:</p> </div>
<div data-bbox="289 1144 748 1182" data-label="Section-Header"> <h3>Direct estimates of production</h3> </div> <div data-bbox="321 1188 703 1218" data-label="Section-Header"> <h4>Using $d(\text{Chl } a)/dt$ to estimate production</h4> </div> <div data-bbox="235 1220 755 1476" data-label="List-Group"> <ul style="list-style-type: none"> • Brown <i>et al.</i> (1985) calculated production during the North Atlantic bloom <ul style="list-style-type: none"> ▶ 4 regions: shelf, slope, Gulf stream and Gulf Stream warm core ring ▶ Assumed C:Chl <i>a</i> ratio and monitored changes in estimated Chl <i>a</i>, with high precision • Abbott and Zion (1985) calculated phytoplankton growth rates in California upwelling region. <ul style="list-style-type: none"> ▶ Used satellite-tracked drogues to estimate time water had traveled between 2 points ▶ assumed difference in satellite-derived Chl <i>a</i> was due to phytoplankton growth </div> <div data-bbox="529 1472 786 1516" data-label="Image"> </div>	<div data-bbox="816 1110 1365 1148" data-label="Section-Header"> <h3>Slide 15 Direct estimates of production</h3> </div> <div data-bbox="816 1232 940 1266" data-label="Text"> <p>NOTES:</p> </div>

Estimating production from CZCS time-series images

Brown *et al.* (1985) estimated high slope production



Temperature

Chl a

Slide 16 Estimating production from CZCS time-series images

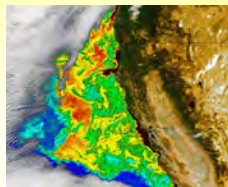
NOTES:

Estimating production from Lagrangian estimates of Chl a

California Sea-surface Chl a

- Abbott and Zion (1985) calculated phytoplankton growth rates in California upwelling region.

- ▶ Used satellite-tracked drogues to estimate time water had traveled between 2 points
- ▶ assumed difference in satellite-derived Chl a was due to phytoplankton growth
- ▶ calculated growth of 0.9 d^{-1}

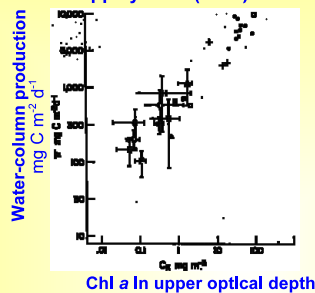


Slide 17 Estimating production from Lagrangian estimates of Chl a

NOTES:

Regression of production on Chl a

Eppley *et al.* (1985): note log-log scale



Slide 18 Regression of production on Chl a

NOTES:

NE Shelf production

Campbell & O'Reilly (1988); NMFS MARMAP data

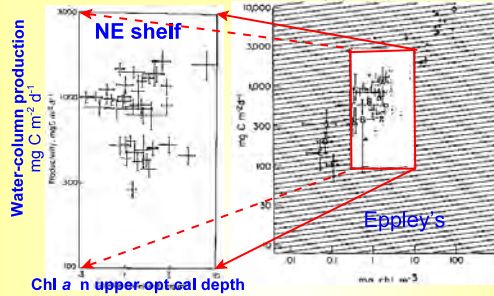


Slide 19 NE Shelf production

NOTES:

Eppley's (1985) relationship weak

Campbell & O'Reilly (1988)

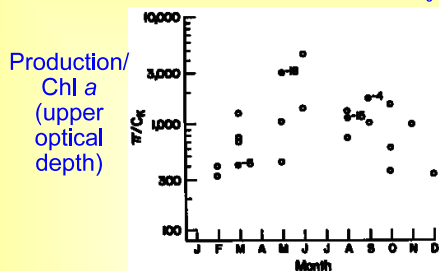


Slide 20 Eppley's (1985) relationship weak

NOTES:

Effects of light on Prod:Chl $a_{(1/k)}$

Eppley *et al.* (1985); higher Chl *a*-specific production in summer. Note the correlation with I_0 .

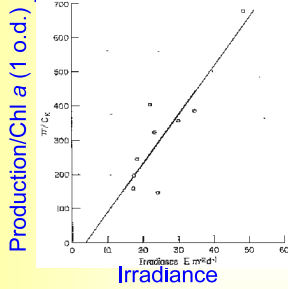


Slide 21 Effects of light on Prod:Chl $a_{(1/k)}$

NOTES:

Eppley/Platt/Cole-Cloern/Malone relationship, later labeled ψ

Eppley *et al.* (1985): linearity between I_0 and production



Slide 22 Eppley/Platt/Cole-Cloern/Malone relationship, later labeled ψ

NOTES:

Cole-Cloern relation for estuaries

Cole & Cloern (1987) $BZ_p I_0$, same as Platt (1986)

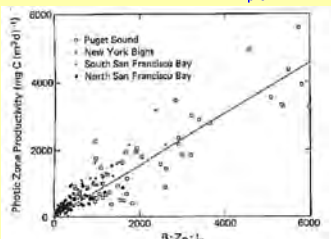


Fig. 2. Regression of photo zone productivity against the composite parameter $BZ_p I_0$ for 211 incubation experiments. $P = 150 + 0.73 (BZ_p I_0)$, $r^2 = 0.82$; S_e (standard error of the estimate) = 410

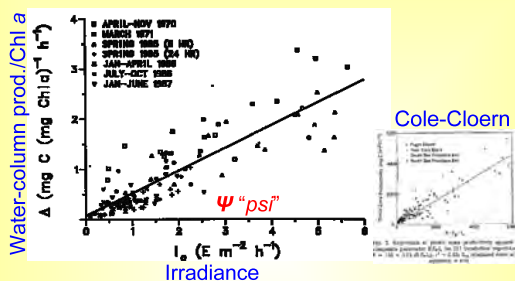
This relationship does NOT rule out nutrient limitation increased nutrient load results in higher Chl *a* ($B \cdot Z_p$)

Slide 23 Cole-Cloern relation for estuaries

NOTES:

Platt's (1986) production algorithm

Extends Eppley *et al.* (1985), same as Cole-Cloern

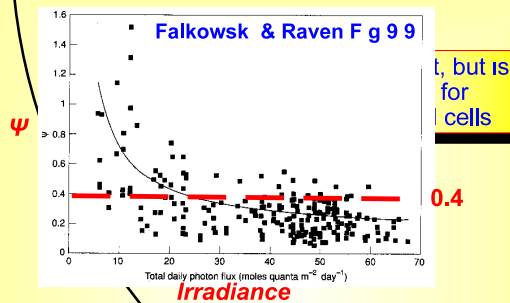


Slide 24 Platt's (1986) production algorithm

NOTES:

Falkowski & Raven (1997)

Platt assumed constant Ψ , but Ψ does vary greatly



Slide 25 Falkowski & Raven (1997)

NOTES:

Estimating production from space with bioptical models

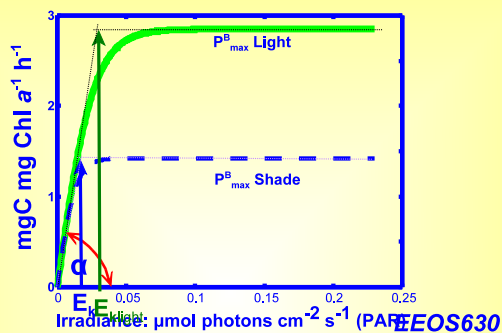
Platt & Sathyandranath's and Behrenfeld & Falkowski's algorithms



Slide 26 Estimating production from space with bioptical models

NOTES:

Estimating Chl profile & P vs. I curve



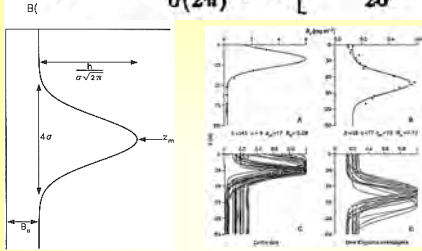
Slide 27

NOTES:

Bio-optical models & SSCM

Platt (1986) & Platt & Sathyendranath (1988)

$$B(z) = B_0 + \frac{h}{\sigma(2\pi)^{1/2}} \exp \left[-\frac{(z - z_m)^2}{2\sigma^2} \right]$$

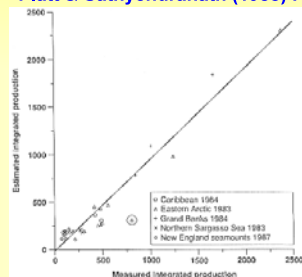


Slide 28 Bio-optical models & SSCM

NOTES:

Estimated vs. measured Production for the North Atlantic

Platt & Sathyendranath (1988) Fig. 1



Slide 29 Estimated vs. measured Production for the North Atlantic

NOTES:

N. Atlantic production

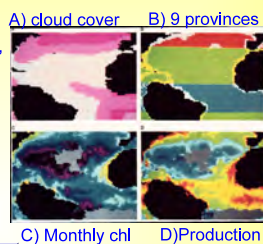
Platt & Sathyendranath (1988) Fig. 3

9 Biogeographic provinces south of 50° N

- Three depth zones: shelf, slope & oceanic
- Three latitudinal zones: equatorial, subtropical & transitional

The parameters needed to characterize the chlorophyll profile estimated from archived data

- 3800 grid points chosen, cloud cover estimated, and productivity profiles estimated

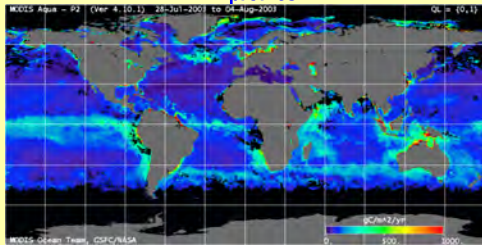


Slide 30 N. Atlantic production

NOTES:

Behrenfeld-Falkowski algorithm

Generalized productivity profiles, 1042 MARMAP profiles



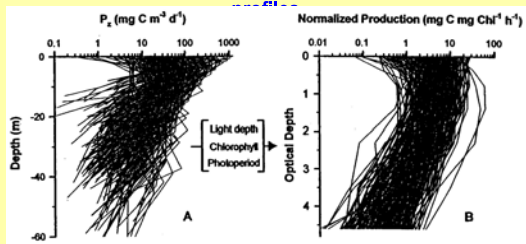
<http://www.science.oregonstate.edu/ocean.productivity/index.php>

Slide 31 Behrenfeld-Falkowski algorithm

NOTES:

Behrenfeld-Falkowski algorithm

Generalized productivity profiles, 1042 MARMAP

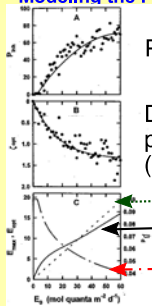


Slide 32 Behrenfeld-Falkowski algorithm

NOTES:

Behrenfeld & Falkowski VGPM

Modeling the P vs. I curve & productivity-depth relation



Photoinhibition

Depth to optimum photosynthesis (optical depths)

Inflection pt in P vs. E curve

Daily PAR at optimum Z

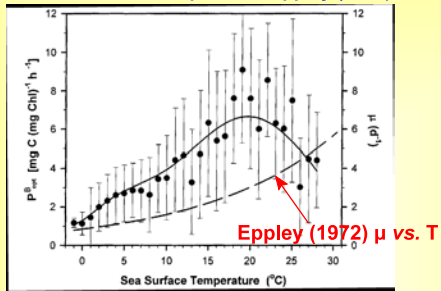
Photoinhibition

Slide 33 Behrenfeld & Falkowski VGPM

NOTES:

Assimilation number as $f(\text{temp})$

Compared to Eppley (1972)

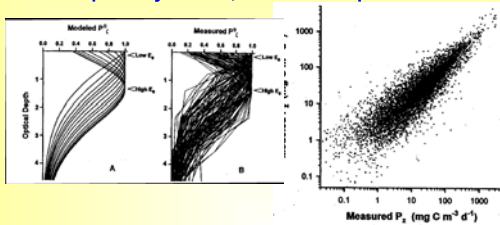


Slide 34 Assimilation number as $f(\text{temp})$

NOTES:

Est. vs. Observed Productivity

$R^2 = 79\%$, Behrenfeld & Falkowski (1997) in gross photosynthesis, 86% of areal production



Slide 35 Est. Vs. Observed Productivity

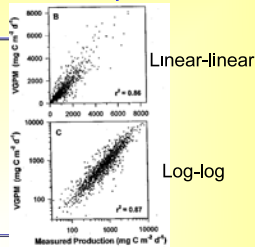
NOTES:

Observed versus modeled areal production

Explains 86-87% of variation in areal production

- Requires knowing or estimating
 - Chl *a* concentration at depth
 - Optimum photosynthetic rate at depth

- These parameters can be estimated from satellite data
 - surface temperature
 - light
 - Chl *a* in upper optical depth



Slide 36 Observed versus modeled areal production

NOTES:

Summary of Behrenfeld & Falkowski algorithm

Joint & Groom (2000)

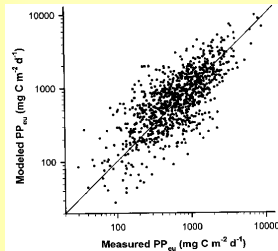
Perhaps the most promising approach to date is the model suggested by Behrenfeld and Falkowski (1997a). This is a light-dependent, depth-independent model which requires a small number of parameters. Depth-integrated primary production, PP_{int} , is estimated from the following: $P^{0.01}$, the maximum rate of chlorophyll-specific carbon fixation in the water column; $I_{0.01}$, sea surface daily photosynthetically available radiation (PAR); $Z_{0.01}$, the depth of water from the surface to where light is 1% of that at the surface; $C_{0.01}$, the chlorophyll concentration at the depth at which $P^{0.01}$ occurs; and D , the number of hours of daylight on that day. This simple model explained 86% of the variance between measured and modelled production estimates for a very large data set of nearly 1700 estimates of primary production from a number of marine provinces. The limitation in this model is that when $P^{0.01}$ was estimated from a parameter available from remote sensing (sea-surface temperature) the variance explained dropped to 58%

Slide 37 Summary of Behrenfeld & Falkowski algorithm

NOTES:

Measured vs. Modeled production

Behrenfeld & Falkowski(1997) Figure 8 with parameters estimated from surface temperature, Chl a in upper optical depth, and light (I_0): $R^2=58\%$



Slide 38 Measured vs. Modeled production

NOTES:

Behrenfeld et al. (2005)

Estimating μ from space

[5] Here we proceed through a sequence of steps that lead from satellite Chl and b_{phy} determinations to global carbon-based estimates of ocean NPP. From b_{phy} , we estimate phytoplankton carbon biomass (C) and then demonstrate that regional satellite Chl:C ratios behave in a manner consistent with well-established physiological dependencies on light, nutrients, and temperature. We then use Chl:C data to estimate phytoplankton growth rates (μ) and, finally, calculate NPP from the product of μ and C. In this manner, closure on the productivity equation is achieved through remote sensing, yielding a new view of global ocean productivity and its variation over space and time.



Slide 39 Behrenfeld et al. (2005)

NOTES:

